Environmental Modelling & Software 26 (2011) 1325–1336

Contents lists available at ScienceDirect

Environmental Modelling & Software

journal homepage: www.elsevier.com/locate/envsoft

Derivation of lake mixing and stratification indices from high-resolution lake buoy data

Jordan S. Read [a], David P. Hamilton [b,*], Ian D. Jones [c], Kohji Muraoka [b], Luke A. Winslow [d], Ryan Kroiss [d], Chin H. Wu [a], Evelyn Gaiser [e]

[a] Department of Civil and Environmental Engineering, University of Wisconsin–Madison, 1415 Engineering Drive, Madison, WI 53706, USA
[b] Centre for Biodiversity and Ecology Research, University of Waikato, Private Bag 3105, Hamilton 3240, New Zealand
[c] Centre for Ecology and Hydrology, Lancaster Environment Centre, Lancaster LA1 4AP, United Kingdom
[d] Center for Limnology, University of Wisconsin–Madison, 680 North Park Street, Madison, WI 53706, USA
[e] Department of Biological Sciences and Southeast Environmental Research Center, Florida International University, FL 33199, USA

ARTICLE INFO

Article history:
Received 6 November 2010
Received in revised form
27 April 2011
Accepted 6 May 2011
Available online 31 May 2011

Keywords:
Lake analyzer
Stability
Mixing
Lake number
Wedderburn number
Schmidt stability
Thermocline depth
Software
Instrumented buoy
GLEON

ABSTRACT

Lake Analyzer is a numerical code coupled with supporting visualization tools for determining indices of mixing and stratification that are critical to the biogeochemical cycles of lakes and reservoirs. Stability indices, including Lake Number, Wedderburn Number, Schmidt Stability, and thermocline depth are calculated according to established literature definitions and returned to the user in a time series format. The program was created for the analysis of high-frequency data collected from instrumented lake buoys, in support of the emerging field of aquatic sensor network science. Available outputs for the Lake Analyzer program are: water temperature (error-checked and/or down-sampled), wind speed (error-checked and/or down-sampled), metalimnion extent (top and bottom), thermocline depth, friction velocity, Lake Number, Wedderburn Number, Schmidt Stability, mode-1 vertical seiche period, and Brunt-Väisälä buoyancy frequency. Secondary outputs for several of these indices delineate the parent thermocline depth (seasonal thermocline) from the shallower secondary or diurnal thermocline. Lake Analyzer provides a program suite and best practices for the comparison of mixing and stratification indices in lakes across gradients of climate, hydro-physiography, and time, and enables a more detailed understanding of the resulting biogeochemical transformations at different spatial and temporal scales.

1. Introduction

Thermal stratification in lake ecosystems exerts an important control on the in-lake vertical fluxes of dissolved and particulate material (Robertson and Imberger, 1994; Aeschbach-Hertig et al., 2007). Stratification is facilitated by the thermal expansion properties of water, which create a stable vertical density gradient owing to heating (or cooling if below 3.98 °C) of surface waters. These density gradients are often observed as a region of sharp change in water temperature (metalimnion) that delineates an upper well-mixed region (epilimnion) from a relatively quiescent deep zone (hypolimnion) (Monismith and MacIntyre, 2009). This vertical partitioning of the water column has important implications for the availability of nutrients, light, and microbial substrates, as well as vertical distribution, migration, and feeding of higher trophic levels like zooplankton and fish. Density stratification suppresses vertical transfer between bottom and surface waters, often resulting in a nutrient rich but light-limited hypolimnion in stark contrast to an epilimnion rich in light but poor in nutrients (MacIntyre et al., 1999). Connectivity between the hypolimnion and the atmosphere is also limited by stratification, which creates a barrier to the replenishment of oxygen (Wetzel, 1983) and the efflux of hypolimnetic carbon (Cole et al., 2007).

Stratification can be transient or persistent, varying at time scales of hours (Rueda and Schladow, 2009) to decades (Jellison et al., 1998; Verburg et al., 2003), finally decaying to near vertical homogeneity as mixing mechanisms such as wind and convection outweigh the stabilizing inputs of surface heating. Lakes range in stratification strength (as measured by the Brunt-Väisälä buoyancy frequency: N^2) by as much as nine orders of magnitude (Wüest and Lorke, 2003), resulting in substantial variations in the energy required to break down stratification. Stratification can therefore

* Corresponding author.
E-mail address: davidh@waikato.ac.nz (D.P. Hamilton).

1364-8152/$ – see front matter © 2011 Elsevier Ltd. All rights reserved.
doi:10.1016/j.envsoft.2011.05.006

vary on global and regional scales as destratifying drivers such as wind follow synoptic patterns but are also affected by local topography (McGowan and Sturman, 1996).

With expanding global coverage of sensor networks (Porter et al., 2009) a large volume of data is rapidly being accumulated for lakes across the world. Lake monitoring networks show promise for addressing science questions that span broad geographic regions and ecosystem gradients, but adequate tools are required to rapidly process this information to contribute towards comparative studies. These studies will benefit from the available gradients of climate, land-use, hydro-physiography, and time that are provided by a global network (Hanson, 2007).

Comparative studies in limnological research that span broad spatial or temporal extents are often limited by the large effort and investment in infrastructure required to conduct large-scale research (Magnuson et al., 1997). The few large comparative surveys that do exist (e.g. Fee et al., 1996) have improved our understanding of physical drivers of ecosystem processes, while highlighting the large amount of variability in space and time. A common, but non-exclusive theme to these large-scale studies is the synthesis of several spatially disparate – often global – data sources, driven by cross-site collaborative efforts (e.g. Magnuson et al., 2000). Barriers to these collaborations have historically been the physical separation of researchers, but recent advances in cyber-tools have helped to simplify global collaborations and reinforce trust (Hanson, 2007). A synchronous increase in deployments of instrumented buoys has led to the unprecedented ability to increase the temporal resolution and spatial extent of comparative lake research (Porter et al., 2009) as these buoys can be used as sentinels for the dynamics of entire eco-regions (Williamson et al., 2009).

Physical indices derived from instrumented buoys can be used to effectively parse out the contributions of drivers like wind (Lake Number; Wedderburn Number), convective cooling (decrease in Schmidt Stability), and destratifying forces that weaken vertical density gradients (decrease in buoyancy frequency) on measured biological signals (e.g. Robertson and Imberger, 1994); but we currently lack standards and best practices for these calculations. These indices of lake behaviour have been well established in the literature, but several nuances persist over the exact definition of ubiquitous concepts such as the extent of the mixed layer or the thermocline depth, hampering our ability for cross-site comparison. For example, depth of the mixed layer has been calculated as a threshold of turbulence (MacIntyre et al., 2009), a temperature gradient (Coloso et al., 2008), a density gradient (Lamont et al., 2004), or chemical gradient (Cole et al., 2000). The current state of aquatic sensor network science stands to benefit from the unification of various methods used in the calculation of physical indices of biogeochemical processes, allowing more robust conclusions and future synthesis. We therefore require a consistent methodology which is robust over many types of lakes and is easily applied to data from lake monitoring buoys. We present here a numerical scheme and accompanying program suite specifically designed for data-rich aquatic sensor networks. Our software package is founded on robust and unified methods, establishing a physical basis for future biogeochemical studies in a simplified framework. This assemblage of open-source tools is unprecedented in the field of sensor network science, and provides a basis for scientific advancement through transparency and information sharing.

2. Comparative indices

The following methods for calculating lake-specific indices offer an approach which is consistent with the existing literature and has been specifically designed to accommodate the sensor arrays of instrumented lake buoys. As instruments are most commonly referenced from a floating surface-mounted buoy, we employ a coordinate system frequently used by the limnological community, but which differs from established physical literature (e.g. Imberger, 1985; Wüest and Lorke, 2003), as we treat the air/water interface as depth 0 with positive z in the downward direction. Lake Analyzer can be used for calculation of the extent of the metalimnion (top and bottom), the depth of the thermocline, Schmidt Stability, Wedderburn Number, Lake Number and the Brunt-Väisälä buoyancy frequency, as well as other related parameters (as detailed in Sections 2.1–2.5 and A.1).

2.1. Thermocline/pycnocline depth

The depth to the thermocline has been used as a climate change indicator, or to show lake response to coupled changes in heat budget and mixing dynamics. Hambright et al. (1994) for example, calculated changes in thermocline depth for Lake Kinneret (Israel) over a period of 23 years (1969–1990), using a scheme based on the maximum change in temperature with respect to change in depth. Because temperature measurements are taken at discrete intervals, the vertical resolution of thermocline estimates has typically been limited by the resolution of the measurements. This methodology presents an issue of "steps" in a time series of thermocline estimates, often incorrectly representing a gradual lowering of the thermocline depth with a series of sharp drops. To minimize this issue, we present a scheme designed to improve this discretized method by adding weighting to adjacent measurements:

Water density (ρ) is calculated according to the contributions of temperature and solutes (if applicable) (Fig. 1a and b; see A.1.1). For k number of measurements referenced from the surface, for $i = 1$ to $i = k - 1$:

$$\frac{\partial \rho}{\partial z_{i\Delta}} = \frac{\rho_{i+1} - \rho_i}{z_{i+1} - z_i}, \tag{1}$$

which applies to the depth characterized by $z_{i\Delta} = (z_{i+1} + z_i)/2$, where $z_{i\Delta}$ represents a midpoint depth between measurements i and $i + 1$. If the maximum $\partial\rho/\partial z_{i\Delta}$ is found when $i = \zeta$ for discrete measurements (Fig. 1c), the true depth of the maximum change in density (z_T) likely occurs within the bounds defined by the two depths at which the discrete measurements were taken ($z_\zeta < z_T < z_{\zeta+1}$). An improvement on the initial guess of $z_T \approx z_{\zeta\Delta}$ can be made by weighting the magnitudes of the difference between the maximum calculated density change and the adjacent calculations (Fig. 1c and d);

$$z_T \approx z_{\zeta+1}\left(\frac{\Delta\rho_{+1}}{\Delta\rho_{-1} + \Delta\rho_{+1}}\right) + z_\zeta\left(\frac{\Delta\rho_{-1}}{\Delta\rho_{-1} + \Delta\rho_{+1}}\right) \tag{2}$$

Crystal Lake conductivity-temperature-depth (CTD) casts, where $(z_{\zeta\Delta+1} - z_{\zeta\Delta})/(\partial\rho/\partial z_{\zeta\Delta} - \partial\rho/\partial z_{\zeta\Delta+1})$ has been simplified to $\Delta\rho_{+1}$ and $(z_{\zeta\Delta} - z_{\zeta\Delta-1})/(\partial\rho/\partial z_{\zeta\Delta} - \partial\rho/\partial z_{\zeta\Delta-1})$ to $\Delta\rho_{-1}$. This scheme shows a potential improvement in accuracy over existing methods when compared to known density profiles (for Crystal Lake conductivity-temperature-depth (CTD) casts, 39% reduction in average error for 1 m intervals and 18% reduction in average error for 2 m intervals: Fig. 2). The same relationship can be used to estimate the maximum change in temperature with respect to depth (a decreasing gradient when $T > 3.98$ °C), but we focus here on the density gradient because it holds more physical relevance to the suppression of vertical mixing. Because of the significance of both the parent and secondary thermocline (e.g. Kling, 1988), we include a scheme that allows the output of either (or both) of these estimates (see A.1.2).

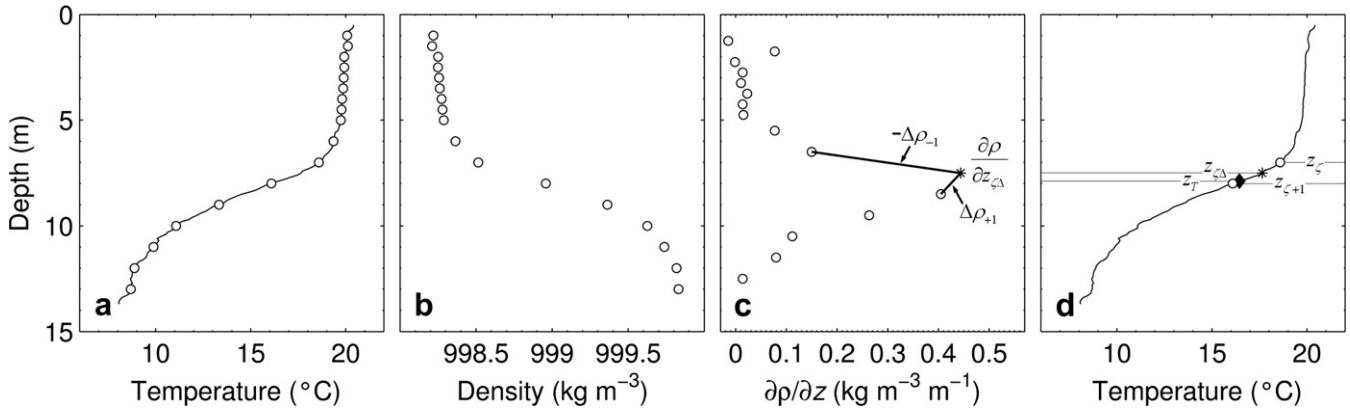

Fig. 1. Algorithm for estimating the thermocline/pycnocline depth from example data. (a) Continuous thermal profile (CTD cast, 10 cm resolution; thin black line) sampled at 0.5 m intervals (1–5 m) and 1 m intervals (5–14 m) to simulate discrete buoy thermistor measurements (○). (b) Discrete temperature measurements from (a) converted into water density. (c) Changes in density with respect to changes in depth ($\partial\rho/\partial z$) for discrete measurements. Maximum change is shown as ✳. Lake Analyzer's thermocline uses weighting from adjacent calculations (slopes shown as $\Delta\rho_{-1}$ and $\Delta\rho_{+1}$) to improve upon the discrete maximum (✳). (d) Original temperature profile from (a) with thermocline depth estimate (◆; z_T), calculation boundaries (○; z_ζ and $z_{\zeta+1}$), and discrete maximum (✳; $z_{\zeta\Delta}$).

2.2. Mixed layer depth

Imberger (1985) defined the surface mixed layer as the vertical portion of the water column which is directly influenced by the surface drivers of wind and convective cooling. The upper boundary of this layer is the air/water interface, while the bottom is defined as a threshold between active and transient turbulence. Because most instrumented lakes lack direct measurements of turbulence, it is usually assumed that the mixed layer will be relatively vertically homogeneous in both temperature and density, owing to active mixing. This assumption leads to a partitioning of the mixed layer based on the lack of vertical gradients in temperature and density. Lamont et al. (2004) for example, defined the mixed layer as the region above the thermocline where the density gradient was less than 0.5 kg m^{-3} per metre, while Fee et al. (1996) defined the layer as the region where the temperature gradient is less than 1 °C m^{-1}. Similar to Lamont et al. (2004), the scheme we have chosen relies on a density gradient threshold ($\delta_{\min}$) to define the depth of the mixed layer. Calculations of the density gradient ($\partial\rho/\partial z$) are based on discrete thermistor locations, and the depth of the lower boundary of the mixed layer can be estimated by linear interpolation of the slopes derived from Eq. (1) (Fig. 3). This numerical scheme can be described as (following the notation in Section 2.1): from $i = \zeta$ to $i = 1$, find i where $\partial\rho/\partial z_{i\Delta} \leq \delta_{\min}$, interpolate between i and i+1 to yield the approximate depth of the base of the mixed layer, z_e (also referred to as the top of the metalimnion)

$$z_e = z_{i\Delta} + \left(\delta_{\min} - \frac{\partial\rho}{\partial z_{i\Delta}}\right) \frac{z_{i\Delta} - z_{i\Delta+1}}{\frac{\partial\rho}{\partial z_{i\Delta}} - \frac{\partial\rho}{\partial z_{i\Delta+1}}} \tag{3}$$

Likewise, for the base of the metalimnion, z_h (the theoretical division between the metalimnion and the hypolimnion), from $i = \zeta$ to $i = k - 1$, find i where $\partial\rho/\partial z_{i\Delta} \leq \delta_{\min}$, interpolate between $i - 1$ and i:

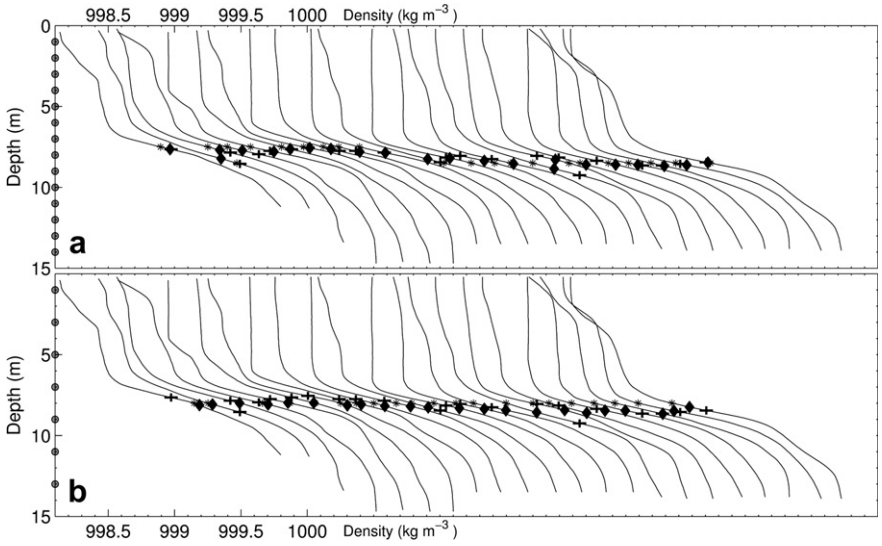

Fig. 2. Thermocline algorithm for 24 days of CTD casts from Crystal Lake, WI, USA, converted to water density (thin black lines, smoothed using a 0.5 m running average from 10 cm measurements). Casts are offset by 0.2 kg m^{-3} on the x-axis for each day. (a) CTD measurements are discretely sampled at 1 m intervals (●), and ✳ represents the maximum discrete change in density, while ◆ is the Lake Analyzer estimate (see Fig. 1; 2.1.2). Actual maximum change in density (✚) is calculated with knowledge of the continuous profile, and error between estimates and actual is taken as the absolute vertical distance between the two. Average error for ✳ was 22.9 cm over all 24 days, with a maximum single day error of 75 cm. Average error for ◆ was 13.9 cm, with a maximum single day error of 44.4 cm. (b) Same as (a), but with 2 m resolution on discrete sampling (●). Average error for ✳ was 32.5 cm, with a maximum single day error of 125 cm. Average error for ◆ was 26.7 cm over all 24 days, with a maximum single day error of 68.2 cm.

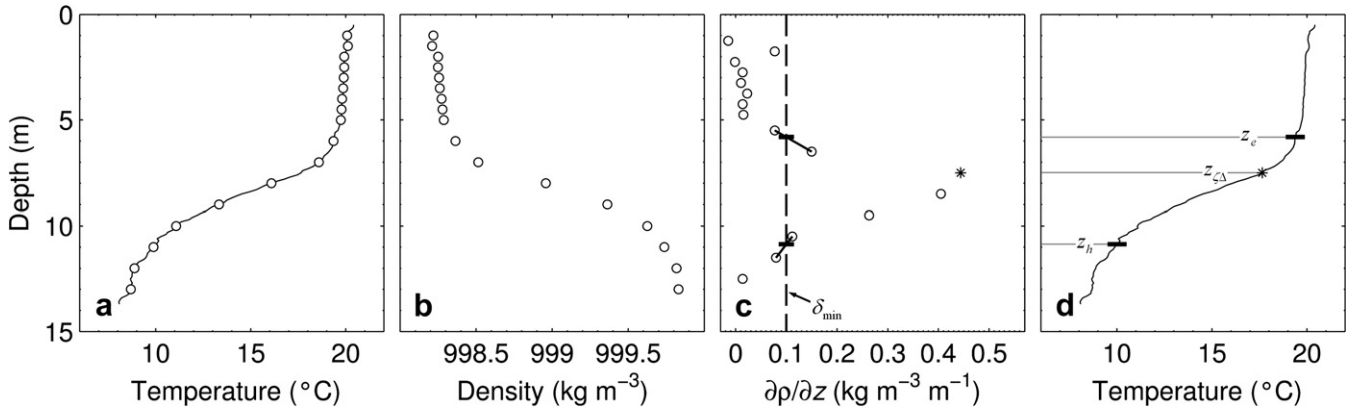

Fig. 3. Algorithm for estimating the extent of the metalimnion (top and bottom) from example data. (a) Same as Fig. 1a. (b) Same as Fig. 1b. Casts started on 20 July 2009, and were completed within 1 h from 17:00 on each day. (c) Moving away from the maximum discrete change in density (from ✳ upward for z_e, downward for z_h), metalimnion top and bottom are estimated by linear interpolation between discrete density changes (○) to a user-specified threshold (δ_{min}). (c) Original temperature profile from (a) with metalimnion top estimate (▬; z_e), metalimnion bottom (▬; z_h), and discrete maximum (✳; $z_{\zeta\Delta}$).

$$z_h = z_{i\Delta-1} + \left(\delta_{\min} - \frac{\partial\rho}{\partial z_{i\Delta-1}}\right) \frac{z_{i\Delta} - z_{i\Delta-1}}{\frac{\partial\rho}{\partial z_{i\Delta}} - \frac{\partial\rho}{\partial z_{i\Delta-1}}} \tag{4}$$

The searching algorithm used to perform these calculations (Eqs. (3) and (4)) requires knowledge of the pycnocline index (ζ from Section 2.1), and searches upward towards the water surface from ζ to find the depth of the top of the metalimnion, and downward towards the lake bottom from ζ to find the depth of the base of the metalimnion (Fig. 3). As in Section 2.1, the Lake Analyzer program allows the calculation of metalimnion bounds relative to the parent or secondary thermoclines (see A.1.2).

2.3. Schmidt stability

The resistance to mechanical mixing due to the potential energy inherent in the stratification of the water column was first defined by Schmidt (1928) and later modified by Hutchinson (1957). This stability index was formalized by Idso (1973) to reduce the effects of lake volume on the calculation (resulting in a mixing energy requirement per unit area). Various authors have adopted Idso's methodology; Kling (1988) for example, found a range of stability of 0–5784 J m^{-2} across 39 West African lakes, while Ferris and Burton (1988) used Schmidt Stability to compare seasonal dynamics in Deep Lake, a hypersaline lake in Antartica. We present Idso's version of Schmidt Stability here as

$$S_T = \frac{g}{A_s} \int_0^{z_D} (z - z_v)\rho_z A_z \partial z \tag{5}$$

where g is the acceleration due to gravity, A_s is the surface area of the lake, A_z is the area of the lake at depth z, z_D is the maximum depth of the lake, and z_v is the depth to the centre of volume of the lake, written as $z_v = \int_0^{z_D} zA_z\partial z / \int_0^{z_D} A_z\partial z$.

2.4. Wedderburn Number

The Wedderburn Number (W), was introduced by Thompson and Imberger (1980) to describe the likelihood of upwelling events under stratified conditions. For $W \leq 1$ there is a high probability that the thermocline will tilt to the surface at the upwind end of the lake and metalimnetic water will be entrained into the surface mixing layer, causing an increase in mixed layer depth; otherwise ($W > 1$) the mixed layer will deepen slowly (Imberger and Patterson, 1990). W has frequently been used as a parameter to describe potential upwelling events in lakes (e.g. Stevens and Lawrence, 1997; MacIntyre et al., 2002; Lamont et al., 2004; Shintani et al., 2010). The Wedderburn Number can be written as

$$W = \frac{g' z_e^2}{u_*^2 L_s} \tag{6}$$

where $g' = g \cdot \Delta\rho/\rho_h$ is the reduced gravity due to the change in density ($\Delta\rho$) between the hypolimnion (ρ_h) and epilimnion (ρ_e), z_e is the depth to the base of the mixed layer (Eq. (3)), L_s is the lake fetch length and u_* is the water friction velocity due to wind stress (A.1.3, Eq. (9)).

2.5. Lake Number

The Lake Number (L_N), defined by Imberger and Patterson (1990), has been used to describe processes relevant to the internal mixing of lakes induced by wind forcings. As with W, lower values of L_N represent a higher potential for increased diapycnal mixing, which increases the vertical flux of mass and energy across the metalimnion through the action of non-linear internal waves (MacIntyre and Melack, 2009). It has been used, for example, to estimate the flux of oxygen across the thermocline in a small lake (Robertson and Imberger, 1994), and to explain the magnitude of the vertical flux of ammonium in a lake (Romero et al., 1998). Lake Number is given by

$$L_N = \frac{S_T(z_e + z_h)}{2\rho_h u_*^2 A_s^{1/2} z_v} \tag{7}$$

where z_e and z_h are the depths to the top and bottom of the metalimnion, respectively (Eqs. (3) and (4)).

3. Materials and methods

Lake Analyzer is a numerical program suite and supporting visualization tools for the calculation of indices of mixing and stratification in lakes and reservoirs. These physical indices are calculated according to established literature with a time series output format. The Lake Analyzer program was created for the rapid analysis of large volumes of high-frequency data collected from instrumented lake buoys (Tables 1 and 2).

Table 1
Key physical parameters used in this text.

Property	Units	Description
A_z	m^2	Lake area at depth z
$\Delta\rho$	kg m^{-3}	Difference in density between epilimnion and hypolimnion
$\partial\rho/\partial z$	kg m^{-3} m^{-1}	Vertical density gradient
$\partial\rho/\partial z_{i\Delta}$	kg m^{-3} m^{-1}	Vertical density gradient between measurements at i and $i+1$
g	m s^{-2}	Acceleration due to gravity
g'	m s^{-2}	Reduced gravity
i	–	Depth index
k	–	Total number of thermistors
κ	–	von Karman constant
L_N	–	Lake Number
L_s	m	Lake length at the water surface
L_T	m	Lake length at the depth of the thermocline
L_z	m	Lake length at depth z
N^2	s^{-2}	Local stability of the water column (buoyancy frequency)
ρ_{air}	kg m^{-3}	Density of air
ρ_e	kg m^{-3}	Average density of the epilimnion (surface mixed layer)
ρ_h	kg m^{-3}	Average density of the hypolimnion
ρ_i	kg m^{-3}	Water density at measurement 'i'
ρ_0	kg m^{-3}	Average density of the water column
S_i	–	Salinity at measurement 'i'
δ_{min}	kg m^{-3} m^{-1}	Threshold for metalimnion bounds
S_T	J m^{-2}	Schmidt stability (Idso, 1973)
S_{t^*}	kg m	Schmidt stability used in L_N calculation
τ_w	N m^{-2}	Surface wind shear stress
T_i	°C	Water temperature at measurement 'i'
T_{mix}	°C	Top to bottom temperature differential for "mixed" condition
u^*	m s^{-1}	Water friction velocity
W	–	Wedderburn Number
U	m s^{-1}	Wind speed at 10 m above the water surface
U_z	m s^{-1}	Wind speed at height z above the water surface
z_e	m	Depth to the top of the metalimnion
z_h	m	Depth to the bottom of the metalimnion
z_i	m	Depth of measurement i (downward positive)
$z_{i\Delta}$	m	Midpoint depth between z_i and z_{i+1}
z_ζ	m	Depth of maximum discrete density gradient
z_T	m	Depth to maximum density gradient
z_v	m	Depth to the centre of volume of the lake
z_D	m	Depth to the bottom of the lake

3.1. Program structure

The Lake Analyzer program suite allows a user to specify desired outputs (such as Lake Number or the depth to the bottom of the mixed layer), and structures the program flow based on these outputs (Fig. 4). This allows the program to be flexible to different data sources, instead of rigidly requiring all potential data files or functions for each program run. This flexible structure increases program speed when only a subset of outputs are selected, and also allows users with data limitations to use the program (as Schmidt Stability, for example, can be calculated without wind speed measurements). The structure of the program is defined by the user output requirements in the .lke *configuration file* (A.2.1), and is adapted to avoid the overhead of redundant calculations or files.

3.2. Program flow

After the program workflow is established by the *program constructor* from the .lke *configuration file*, *primary functions* are called, which then call *secondary functions* and/or trigger the opening of *data files* (.wtr, .wnd, .sal, or .bth), if necessary (Fig. 4). The results from *primary functions* are then organized into a text output file and/or visualized using plotting defaults (see A.2.1.9 and A.2.1.10 for details). Details for each function can be found in Section 2, while additional supporting calculations are explained in A.1.

Table 2
Output options and definitions.

Output	Units	Description
Ln	–	Lake Number
metaB	m	Bottom of the metalimnion depth (from the surface)
metaT	m	Top of the metalimnion depth
N2	s^{-2}	Buoyancy frequency
SLn	–	Seasonal Lake Number
SmetaB	m	Bottom of the seasonal metalimnion depth
SmetaT	m	Top of the seasonal metalimnion depth
SN2	s^{-2}	Seasonal buoyancy frequency
St	J m^{-2}	Schmidt stability (Idso, 1973)
ST1	s	Seasonal mode-1 vertical seiche period
SthermD	m	Seasonal thermocline depth
SuSt	m s^{-1}	Seasonal u-star
SW	–	Seasonal Wedderburn number
T1	s	Mode-1 vertical seiche period
thermD	m	Thermocline depth
uSt	m s^{-1}	u-star (water friction velocity due to wind stress)
W	–	Wedderburn number
wndSpd	m s^{-1}	Wind speed
wTemp	m s^{-1}	Water temperature

3.3. Data sources

Data requirements for Lake Analyzer vary based on the user defined output selections (see Section 3.1), but every Lake Analyzer program run requires either the creation of, or the use of an existing .lke file, which is used to create the program structure. Additional files (.wtr, .wnd) hold time series data of water and wind speed measurements, while a .bth file holds observations of bathymetric areas with respect to depth. An optional input file which holds salinity measurements (.sal) can also be used to improve the density calculations of water, although these effects are ignored if this file is not present. All data source files are simple tab-delimited ASCII text files, with file extensions altered (e.g. .txt changed to .wnd) to facilitate pointer functions in the Lake Analyzer program. See lakeanalyzer.gleonrcn.org for a more detailed user manual for Lake Analyzer.

4. Results

Data are shown for three example lakes, covering a range of size, geographic location and typical stability to illustrate the robustness of the Lake Analyzer Program.

4.1. Lake Annie, Florida (USA)

An example program output for Lake Annie, a subtropical, warm monomictic sinkhole lake (27.21°N, 81.35°W, 19 m maximum depth, 37 ha surface area; see Gaiser et al., 2009 for additional details) is shown in Fig. 5. Measurements of wind speeds and water temperatures were sampled from sensors on 15 min intervals, and were used in raw format (no error checking or down-sampling) to create .wnd and .wtr *data files* (Fig. 4). Fig. 5a is the water temperature ('wTemp') output with thermocline depth outputs ('thermD' and 'SthermD') overlaid. The output resolution for this example Lake Analyzer run was 6 h (.lke {2} = 21600). The effects of a tropical storm (Tropical Storm Fay, see Landsea et al., 2010) were notable in mid-August, as surface water temperatures decreased by approximately 3 °C within hours of the storm, and thermocline depth increased by more than 2 m. Transient stratification patterns of heating and cooling are also evident during winter mixing in late

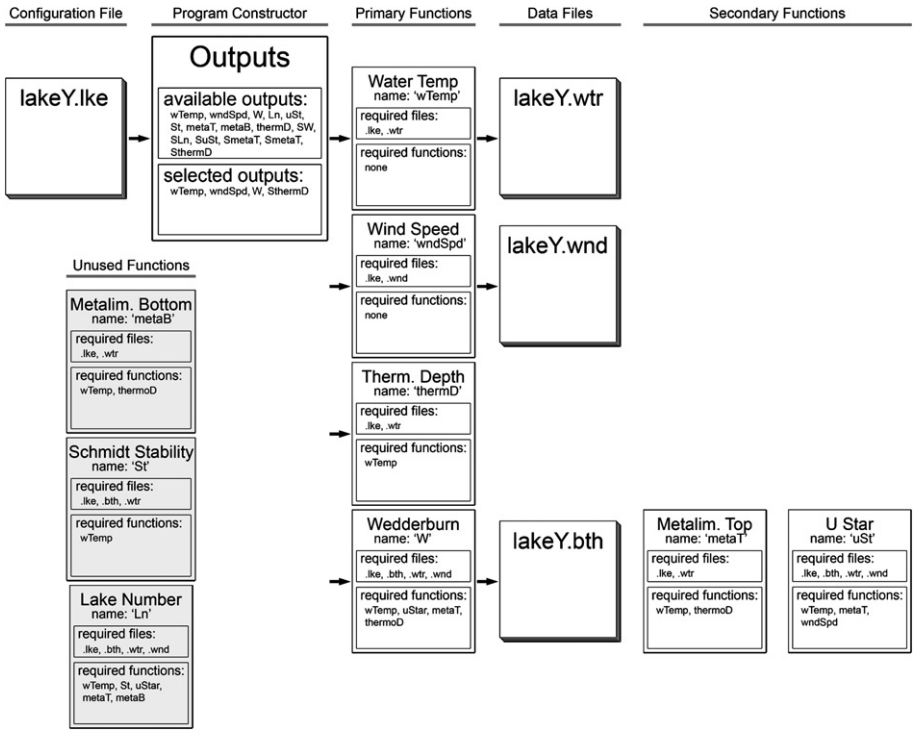

Fig. 4. An example workflow of the Lake Analyzer program (only partial outputs are used here to highlight flexibility of the program structure). The *configuration file* specifies the structure of the program flow, based on user input for desired program outputs (see A.2.2.1). The *configuration file* has the specific extension .lke, with the file name common to source files (such as clearLake.lke, clearLake.wtr, etc.). The *program constructor* assembles the Lake Analyzer program structure through a series of logical statements based on output requirements and function needs. *Primary functions* are direct functions relative to the user-specified outputs. *Data files* are the data sources required for the program run (.wtr, .wnd, and .bth; see A.2.2.2–A.2.2.4). *Data file* .sal is not shown here because it is an optional input file which is not required for the program to run. *Secondary functions* are functions called by primary functions if required as part of the *primary function* output. *Unused functions* are shown here (gray overlay) as functions that are not called during this example workflow.

December into March 2009. Fig. 5b shows the Wedderburn Number and Lake Number, based on the seasonal thermocline (outputs defined by 'SW' and 'SLn', respectively). Both of these dimensionless indices are used to explain the potential for diapycnal mixing events, but the Wedderburn Number displays a higher amount of variability when compared to Lake Number. While W is dependent on the highly variable mixed layer depth (Eq. (6)), L_N relies on the depth to midpoint of the metalimnion (Eq. (7)), which tends to

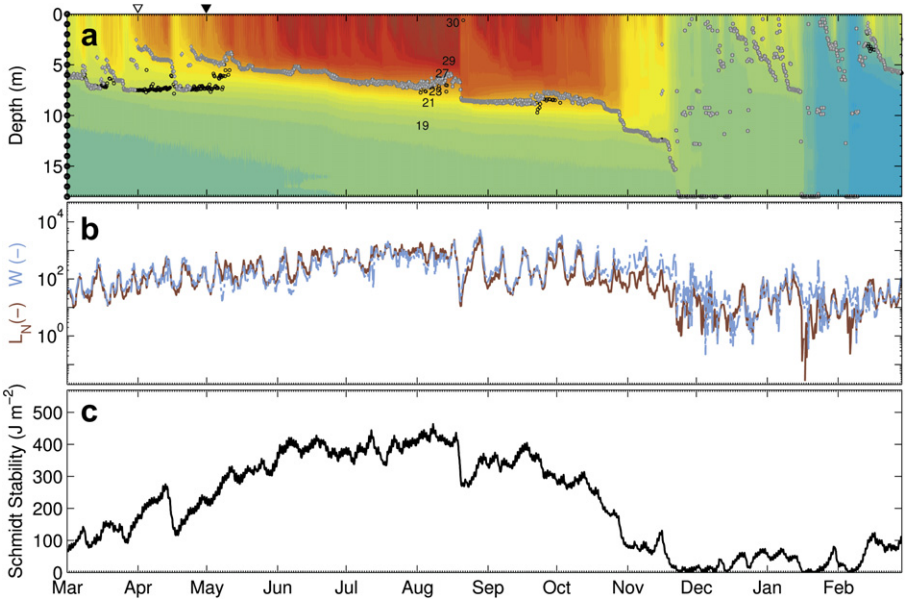

Fig. 5. Program output for Lake Annie, Florida (USA) beginning in 2008. (a) Temperature plot ('wTemp': colors) with color divisions every 0.5 °C (buoy thermistors are shown on left edge: ◍). Seasonal thermocline and maximum gradient thermocline are overlaid ('SthermD', ○ and 'thermD', ◇). (b) Seasonal Wedderburn number ('SW', light blue dashed line) and seasonal Lake Number ('SLN', dark red line) for the same period. (c) Schmidt stability ('St'). (For interpretation of the references to colour in this figure legend, the reader is referred to the web version of this article).

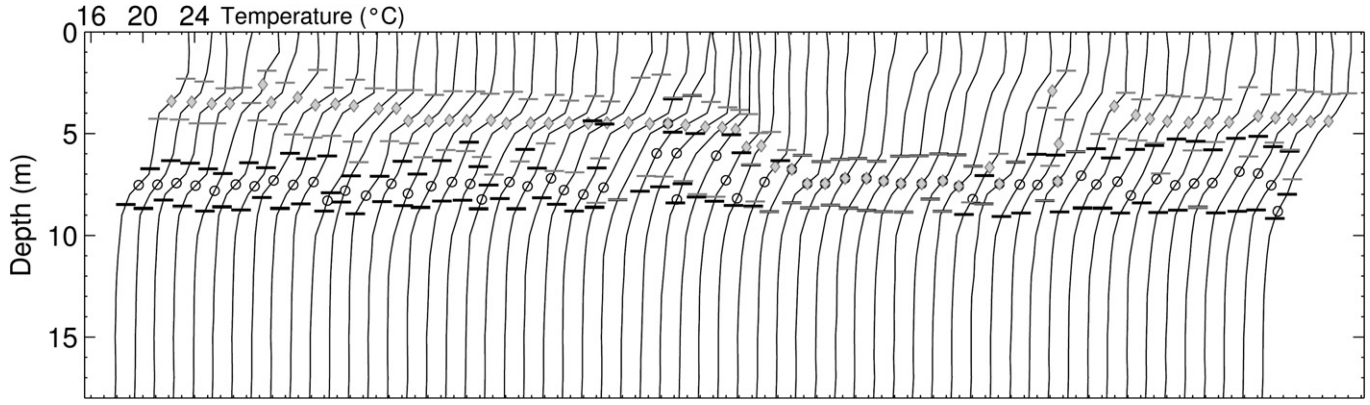

Fig. 6. Thermal profiles taken every 12 h from 1 April 2008 to 1 May 2008 on Lake Annie (see Fig. 5a: ∇ to ▼) offset 1.5 °C on the *x*-axis (thin black lines, taken from 'wTemp' discrete buoy measurements). Seasonal thermocline ('SthermD', ○), maximum gradient thermocline ('thermD', ◇), seasonal metalimnion top and bottom ('SmetaT', ▬; 'SmetaB', ▬), and maximum gradient metalimnion top and bottom ('metaT', ▬; 'metaB', ▬) are shown for each profile.

reduce variability through averaging with the more stable base of the metalimnion. Schmidt Stability is shown in Fig. 5c, where diel patterns in stability are evident as day–night oscillations driven by alternating periods of heating and cooling. The cooling events that increase the depth of the thermocline in mid-April as well as the effects of the mid-August tropical storm are shown clearly as sudden reductions in Schmidt Stability. Lake Annie has periods of transient stratification, where surface heating with limited mixing inputs leads to the formation of a secondary near-surface thermocline. Fig. 6 highlights the difference between outputs based on the parent thermocline ('SthermD') and the maximum gradient thermocline ('thermD') for the period of 1 April to 1 May 2008 on Lake Annie. Water temperature profiles show the merging of the shallower thermocline with the parent thermocline (33rd profile; 17 May), and the establishment of an additional near-surface thermocline (46th profile; 24 May). Depending on the application required by the Lake Analyzer user, parent thermocline (denoted by an 'S' in front of applicable output selections, see A.2.1.11) or maximum gradient thermocline (A.2.1.1–A.2.1.10) can be used.

4.2. Lake Rotorua, Bay of Plenty (NZ)

An example program output for Lake Rotorua, a volcanic crater (38.1°S, 176.3°E 22 m maximum depth (central lake), 79 km^2 surface area, see Burger et al., 2008 for additional details) is shown in Fig. 7. Input data for Lake Rotorua were generated with an instrumented buoy sampled at 30 min intervals from 20 May 2008 to 6 April 2009. Selected outputs and output resolution are the same as for Fig. 5. Lake Rotorua is typically well-mixed, with short periods of defined stratification lasting seldom longer than a week before convective and wind-driven destratification events restore near-isothermal conditions (Fig. 7a). Lake Rotorua's lack of stratification leads to Wedderburn Number and Lake Number values typically below 1 (Fig. 7b), representing a high likelihood of substantial diapycnal fluxes. Schmidt Stability reflects near-isothermal conditions with values close to 0, but (southern hemisphere) summer-time periods of stratification are evident as larger positive values in December 2008 to March 2009 (Fig. 7c). Compared to Lake Annie, Lake Rotorua is much larger (7900 vs.

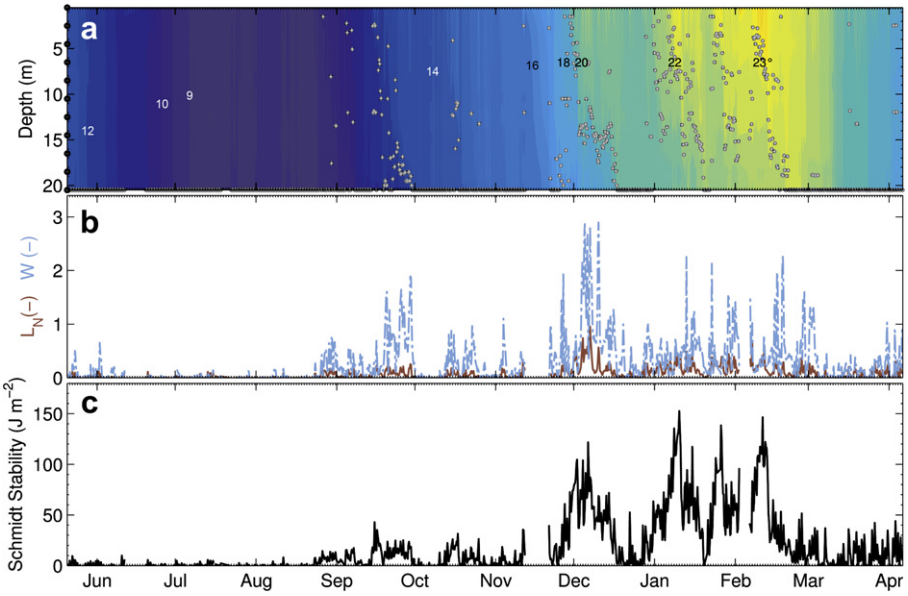

Fig. 7. Same as Fig. 5, but for Lake Rotorua (NZ) starting in 2008.

37 ha), and because of increased wind mixing due to a larger fetch and differences in both climate and latitude (MacIntyre and Melack, 2009), Wedderburn Number and Lake Number are much lower in the Lake Rotorua dataset.

4.3. Lake Mendota, Wisconsin

Metalimnion dynamics for Lake Mendota (43.0°N, 89.42°W, 24 m maximum depth, 3940 ha surface area; see Robertson and Ragotzkie, 1990 for additional details) are shown for the stratified period of 2009 in Fig. 8 (outputs 'wTemp', 'SmetaT', and 'SmetaB'). These results were obtained using the Lake Analyzer program with a specified output resolution of 1 h (.lke {2} = 3600, see A.2.2.1) from buoy thermistor data sampled at 1 min intervals. The presence of internal waves is visible on this higher frequency analysis, as internal seiches can be seen as the coupled oscillations of the metalimnion top and bottom (Fig. 8a). Using the outputs for seasonal metalimnion ('SmetaT', and 'SmetaB' as opposed to 'metaT' and 'metaB') allowed the parent metalimnion to be accurately resolved even during periods of strong surface heating (e.g. mid-September 2009). The thickness of the metalimnion, calculated as the difference between the outputs of 'SmetaB' and 'SmetaT', also shows seasonal dynamics related to surface forcings, as the peak thickness is found during late summer (mid-August) when stratification is greatest (Fig. 8b). Conversely, periods of cooling resulted in thinning of the metalimnion (late September–October 2009), while deepening the surface mixed layer.

5. Discussion

The methods outlined above have been used to create a set of standards and best practices for the calculation of physical indices of stratification – such as Wedderburn Number, Lake Number, and Schmidt Stability – and have been collated into a complete open-source program suite called "Lake Analyzer." This program establishes a framework for the analysis of high-frequency instrumented buoy data, specifically designed for the rapid analysis of large datasets. The Lake Analyzer program provides a much needed analytical tool for the expanding global network of instrumented lakes, where available data is currently increasing at a rate that exceeds scientific output (see GLEON: Hanson, 2007). Data-rich research can benefit from powerful tools like wavelet and time series analyses, which require researchers to combine high-resolution indicators of state with driver and response variables on the same time scales (Moberg et al., 2005; Hanson et al., 2006). Use of these cutting-edge analytical tools is facilitated by the creation of Lake Analyzer, which outputs standardized physical state variables in a time series format.

5.1. Program availability

The program Lake Analyzer was developed for the GLEON (Global Lake Ecological Observatory Network: www.gleon.org) community, a grassroots organization centred around scientific collaboration and data sharing to further the understanding and management of lakes. The Lake Analyzer program is free to download (http://code.google.com/p/lakeanalyzer-2/) under the GNU General Public Licence. Running Lake Analyzer on MATLAB requires a minimum version number of MATLAB 7.4 (additional details for computational requirements for versions of MATLAB can be found at http://mathworks.com/). Alternatively, users without access to MATLAB can use GLEON's web interface for Lake Analyzer (http://lakeanalyzer.gleon.org/), which runs Lake Analyzer on a remote server based on user input files and allows users to download results after completion.

5.2. Program performance

Instrumented buoys can output high-resolution measurements that quickly become overwhelmingly data-rich, as one year of data easily surpasses a million data points when multiple sensors are polled every minute. Simple operations like file opening and routine calculations on this type of data can be cumbersome. The Lake Analyzer program was designed to avoid excessive computational expense in comparative science, as the program can digest large datasets on a common personal computer in seconds instead of hours. We tested the program on an Intel i5 2.4 GHz processor with 4 GB of RAM, using 1 min measurements from Lake Mendota taken over a 200-day period from 23 unique depths and 1 wind

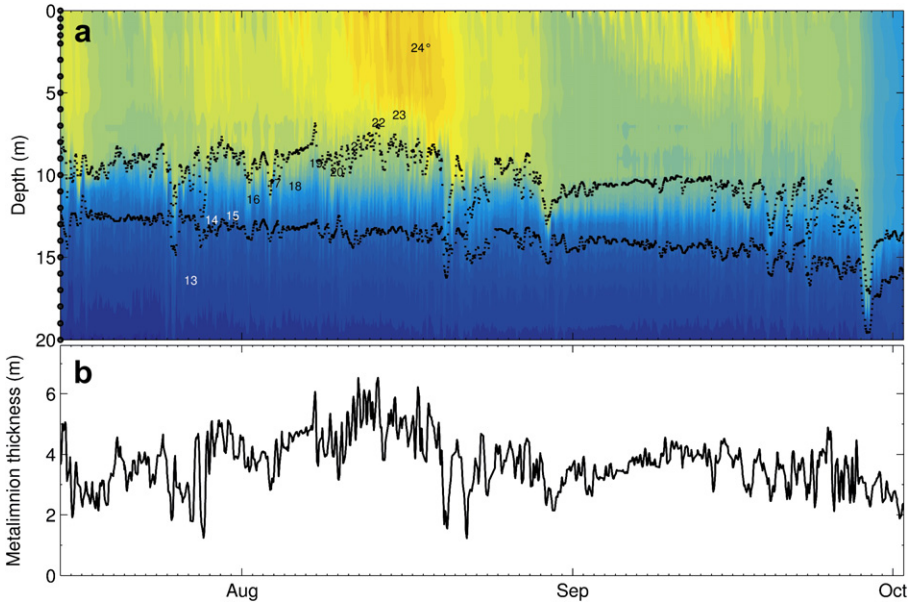

Fig. 8. Metalimnion dynamics for Lake Mendota, Wisconsin (USA) during 2009. (a) Temperature plot ('wTemp', colors) with color divisions every 0.5 °C. Locations of buoy thermistors are shown on right edge (●). Metalimnion bounds for the parent thermocline ('SmetaT' and 'SmetaB', black dots) are overlaid after transforming with a 6 h running average. (b) Thickness of the seasonal metalimnion, taken as the difference between 'SmetaB' and 'Smeta' in metres.

sensor (6,896,496 measurements in 49,052 kB of data files). We simply calculated a time series of Lake Number for each day that was written to a text file and had the program plot the time series. All operations in the program took a total of 33 s, with 60% of this time spent finding and removing sensor errors and 20.6% loading the files. All other time was broken down into much more minor fractions of this total, including the Lake Number calculations.

5.3. Program limitations

The Lake Analyzer program was designed to be robust in the handling of different resolutions of instrumented data, including irregular time intervals. This flexibility adds a layer of user responsibility to the quality of input data, as the program provides limited quality control of the data (limited to error-checking and down-sampling) and assumes that instrument calibration has been performed before creation of input data (or is not needed). Because instrumented buoys vary in vertical and temporal resolution, the user of the Lake Analyzer program should undertake a rigorous quality analysis/quality control program, including error analysis based on the accuracy of sensors and the resolution of the input data. For example, if thermal data is only available at 5 m depth intervals in a highly stratified lake, the accuracy of the thermocline depth and related outputs from the program will suffer compared with measurements made at 1 m intervals (see Fig. 2a and b).

The .lke configuration file gives the user control over error-checking parameters, in addition to effective smoothing ranges (e.g. temporal averaging of layers: .lke {6}, see A.2.2.5). These parameters are designed to increase the utility of the program for both high-resolution applications (Fig. 6a; temporal averaging of layers) and lower-resolution outputs (e.g. Lake Number; see Fig. 5c where epilimnion and hypolimnion layers are averaged over 6 h to reduce the variability due to internal seiches). Lake Analyzer does not provide recommendations for these parameter values, as they are instrument and lake specific. When using Lake Number or Wedderburn Numbers ('Ln', 'SLn', 'W', or 'SW'), we suggest that the user follow the recommendations of MacIntyre et al. (2009) and use temporal averaging of wind and layers of sufficient duration to exceed one-quarter of the first vertical mode internal seiche period (output selection 'T1' or 'ST1').

While Lake Analyzer is limited by a one-dimensional representation of a lake body (as the contributions of horizontal heterogeneity in the wind field, stratification, and basin shape are ignored), future improvements of the program will be a product of the needs and ideas of a diverse body of users, potentially expanding the bounds of some of these restrictions. In the development of Lake Analyzer, we have attempted to maintain a transparent coding structure in an effort to encourage development and further expansion of this useful tool.

6. Conclusions

We have presented a numerical scheme for extracting lake-specific comparative indices of lake stratification and mixing from high-resolution instrumented buoy data, and described some of the potential applications for several of the program outputs. The Lake Analyzer program provides a powerful and easily accessible tool for comparative analyses of lake indices in both time and space, while also including a systematic error-checking algorithm designed for buoy-specific data streams. Any of these tools can be used together for a multiple variable program output, or in any combination to perform specific analyses (such as simply down-sampling and error-checking temperature data). The availability of the program lends it to a high level of transparency for users, as source codes are free to download online. Users without access to the MATLAB scripting language can also use the program on the GLEON online interface (http://lakeanalyzer.gleon.org/), which requires only the proper input files for the analysis. In conclusion, the Lake Analyzer program has been designed to increase the accessibility of physical lake parameters, extending the overlap between ecological and hydrodynamic research, with the intent to facilitate continued collaboration and enable improved data processing.

We thank the Global Lake Ecological Observatory Network (GLEON) and the Archbold Biological Station for working with GLEON to establish the buoy on Lake Annie. We also thank Dale Robertson, Sally MacIntyre, Chris McBride and the GLEON Physics/Climate working group for assisting in the program development, and Paul Hanson and three anonymous reviewers for providing guidance on an earlier version of this manuscript. This work was funded by the National Science Foundation via grants DBI-0446017 and DBI-0639229, in addition to funding provided by the Gordon and Betty Moore Foundation.

A. Appendix

A.1. Additional calculations

A.1.1. Density of water (ρ_i)

Density of water from a given temperature (in °C), assuming negligible effects of any solutes on density, can be calculated as in Martin and McCutcheon (1999) to be:

$$\rho_i = \left[1 - \frac{T_i + 288.9414}{508929.2 \cdot (T_i + 68.12963)}(T_i - 3.9863)^2\right] \cdot 1000 \quad (8a)$$

If solutes are non-negligible and a salinity file (.sal) is provided, density will be calculated according to the combined effects of salinity (S_i) and water temperature based on the methods of Millero and Poisson (1981):

$$\rho_i = \rho_* + A \cdot S_i + B \cdot S_i^{3/2} + C \cdot S_i \quad (8b)$$

where $\rho^* = 999.842594 + 6.793952 \times 10^{-2} \cdot T_i - 9.09529 \times 10^{-3} \cdot T_i^2 + 1.001685 \times 10^{-4} \cdot T_i^3 - 1.120083 \times 10^{-6} \cdot T_i^4 + 6.536336 \times 10^{-9} \cdot T_i^5$,
$A = 8.24493 \times 10^{-1} - 4.0899 \times 10^{-3} \cdot T_i + 7.6438 \times 10^{-5} \cdot T_i^2 - 8.2467 \times 10^{-7} \cdot T_i^3 + 5.3875 \times 10^{-9} \cdot T_i^4$,
$B = -5.72466 \times 10^{-3} + 1.0227 \times 10^{-4} \cdot T_i = 1.6546 \times 10^{-6} \cdot T_i^2$, and
$C = 4.8314 \times 10^{-4}$.

A.1.2. Seasonal thermocline (SthermD)

Lake Analyzer defines the dominant thermocline (*thermD*) as an estimate of the depth of the greatest density change with respect to depth ($\partial\rho/\partial z$). If a secondary local maximum is found in $\partial\rho/\partial z$ at a greater depth than *thermD*, the location of *SthermD* is calculated using Eq. (1). This calculation is not performed (and *SthermD* output will be the same as *thermD*) when either the secondary local maximum is less than 20% of the absolute maximum gradient, or no secondary maximum exists. We found the 20% threshold to work best for a variety of lakes, but users can modify this parameter in the script 'FindThermoDepth.m' by changing the value of 'dRho-Perc', which represents this ratio.

A.1.3. u-star (u_*)

$$u_* = \sqrt{\frac{\tau_w}{\rho_e}} \quad (9)$$

With ρ_e as the average density (kg m^{-3}) of the epilimnion, and τ_w is the wind shear (N m^{-2}) on the water surface, given by

$\tau_w = C_D \rho_{air} U^2$. ρ_{air} is the density of air (kg m^{-3}), and U is wind speed (m s^{-1}) measured at 10 m above the water surface. Wind speed measurements at any height (U_z) other than 10 m (as specified by input #4 in the .lke file) are corrected according to Amorocho and DeVries (1980):

$$U = U_z \left[1 - \frac{C_D^{0.5}}{\kappa} \ln\left(\frac{10}{z}\right) \right]^{-1} \quad (10)$$

where κ is von Karman's constant (taken to be 0.4), z is the height above the water surface for the measurement of U_z. Values for C_D are given by Hicks (1972) as

$C_D = 1 \times 10^{-3}$…for $U < 5$ (m s^{-1})
$C_D = 1.5 \times 10^{-5}$…for $U \geq 5$ (m s^{-1})

A.1.4. Buoyancy frequency (N^2)

$$N^2 = \frac{g}{\rho} \frac{\partial \rho}{\partial z} \quad (11)$$

where N^2 (s^{-2}) represents the local stability of the water column, based on the density gradient $\partial\rho/\partial z$.

A.1.5. Mode-1 vertical seiche period (T_1)

$$T_1 = \frac{2 z_D L_T}{g' z_T (z_D - z_T)} \quad (12)$$

Given by Monismith (1986) where L_T is the basin length at the depth of the thermocline (z_T).

A.1.6. Error-checking of input data

Data from both .wtr and .wnd files are error-checked before being used in any of the calculations. Outliers are removed from the dataset based on two criteria, being greater or less than the maximum and minimum specified range values (A.2.2.7 and A.2.2.8) or being outside 2.5 times the standard deviation of the values within a moving outlier window (A.2.2.6; .lke {7}).

A.1.7. Down-sampling of input data

Data from both .wtr and .wnd files are down-sampled before being used in any of the calculations according to the specified output resolution (A.2.2.1; .lke {1}). If the output resolution is less than the temporal resolution of the input data, down-sampling is not performed on these data. Down-sampled values are temporally averaged values pertaining to the output resolution, i.e. specifying an hourly output resolution (.lke {1} = 3600) for 1 min data will result in hourly data that are each averages of the 60 values that occurred during each hourly period.

A.2. Program variables

For program variables, {n} represents the nth line of the specific input file (i.e. .lke {4} is the 4th line of the .lke file, which contains the height of the wind sensor from the lake surface). These settings specify how the program will be structured.

A.2.1. Outputs

Outputs (.lke {1}) are automatically created in the same directory as the .wtr and .wnd input files, called 'LakeY_results'. Outputs can be entered to the .lke file in any order, but will be written to file according to a pre-determined sequence which can be modified in the 'OutputConstructor.m' source code.

A.2.1.1. wTemp. If wTemp is specified as an output, water temperature (°C) with outlier removal (.lke {8} and {9}) and down-sampling (if output resolution is at least twice the input resolution – .lke {2}) of the input water file is written to file. wTemp is the only output option that creates a separate file in addition to the 'LakeY_results' file, called 'LakeY_results_wtr'.

A.2.1.2. wndSpd. If selected, wind speed (m s^{-1}) is written to the results file, with outlier removal (.lke {10} and {11}), temporal wind averaging (.lke {5}) and down-sampling (where applicable) is applied.

A.2.1.3. metaT. If selected, the depth to the metalimnion top (m) is written to the results file, with temporal layer averaging (.lke {6}) applied. metaT is calculated according to Eq. (2) for time points where the lake is not considered mixed. When the mixed criteria are met (.lke {13}), layers are not calculated, and written to the results file as the maximum depth.

A.2.1.4. metaB. If selected, the depth to the metalimnion bottom (m) is written to the results file, with temporal layer averaging (.lke {6}) applied. metaB is calculated according to Eq. (2) for time points where the lake is not considered mixed. When the mixed criteria are met (.lke {13}), layers are not calculated, and written to the results file as the maximum depth.

A.2.1.5. thermD. If selected, the depth to the thermocline (m) is written to the results file, with temporal layer averaging (.lke {6}) applied. thermD is calculated according to Eq. (1) for time points where the lake is not considered mixed. When the mixed criteria are met (.lke {13}), layers are not calculated, and written to the results file as the maximum depth.

A.2.1.6. St. If selected, Schmidt Stability (J m^{-2}) is calculated by Eq. (5), and written to the results file. Calculations are made with water temperature in the same form as wTemp, even if wTemp is not selected to be written to file.

A.2.1.7. Ln. If selected, Lake Number (dim) is calculated by Eq. (7), and written to the results file. Calculations of Ln are made with wTemp, metaT, metaB, uSt, St.

A.2.1.8. W. If selected, Wedderburn Number (dim) is calculated by Eq. (6), and written to the results file. Calculations of W are made with wTemp, wTemp, metaT, uSt.

A.2.1.9. N2. If selected, the Brunt-Väisälä buoyancy frequency is calculated according to Eq. (11), and written to the results file.

A.2.1.10. T1. If selected, the mode-1 vertical seiche period is calculated according to Eq. (12), and written to the results file.

A.2.1.11. SmetaT, SmetaB, SthermD, SuSt, SLn, SW, SN2, ST1. All as above, with effort to include the parent thermocline (deeper) for all applicable calculations (see A.1.1).

A.2.2. Inputs

A.2.2.1. Output resolution. Output resolution (.lke {2}) specifies the time-step (s) of the calculations made for A.2.1. If the temporal resolution of the input data is coarser than the entry for this input, calculations will be made according to input data resolution.

A.2.2.2. Total depth. Total depth (m) (.lke {3}) must be greater or equal to than the maximum depth given in the .bth file. If the total depth is not included in the .bth file, it is assumed that the area at

total depth is 0 (m^2) and the depth area curve is linearly interpolated from this depth to the values in the .bth file.

A.2.2.3. Height of wind measurement. Height of wind measurement (m) (.lke {4}) is used for the wind speed correction factor in Eq. (11).

A.2.2.4. Wind averaging. Wind averaging (s) (.lke {5}) is the backwards-looking smoothing window used for the calculation of uSt and SuSt. This calculation allows for the relevant wind duration to influence the calculation of wind-derived parameters.

A.2.2.5. Thermal layer averaging. Thermal averaging (s) (.lke {6}) is the smoothing window used for metaT, metaB, thermD, SmetaT, SmetaB, and SthermD. Temporal smoothing for thermal layers is intended to minimize the effects of internal waves on these parameters.

A.2.2.6. Outlier window. Outlier window (s) (.lke {7}) is the window size (seconds) for outlier removal, where measurements outside of the bounds ($\mu \pm 2.2 \cdot \sigma$) based on the standard deviation and the mean inside the outlier window are removed. Outlier removal is performed on .wtr and .wnd files prior to downsampling (if applicable).

A.2.2.7. wtr max, wtr min. Maximum and minimum allowed water temperatures (°C) (.lke {8 and 9}), where all values of .wtr file not fitting this criteria are removed before outlier checking.

A.2.2.8. wnd max, wnd min. Maximum and minimum allowed wind speeds ($m\ s^{-1}$) (.lke {10 and 11}), where all values of .wnd file not fitting this criteria are removed before outlier checking.

A.2.2.9. δ_{min}. Minimum slope for the range of the metalimnion ($kg\ m^{-3}$ per metre) (.lke {12}), which is used to calculated values of metaT, metaB, SmetaT, and SmetaB according to Eq. (2).

A.2.2.10. T_{mix}. Minimum surface to bottom thermistor temperature differential (°C) (.lke {13}) before the case of 'mixed' is applied. When 'mixed' is true, all thermal layer calculations are no longer applicable, and values are given as the depth of the bottom thermistor.

A.2.2.11. Plot figure. Plot figure (Y/N) (.lke {14}) is used to generate and save figure outputs of all calculations selected in .lke {1}. One figure is created for each output, saved at a resolution of 150 dpi. Alterations to figure outputs (resolution and other defaults) can be modified directly in the 'OuputConstructor.m' file.

A.2.2.12. Write results. Write results (Y/N) (.lke {15}) settings are used to determine whether outputs specified in .lke {1} will be written to file. If .lke {14} and {15} are both 'N', the program will alert users that no usable output will be generated, and the program will terminate.

References

Amorocho, J., DeVries, J.J., 1980. A new evaluation of the wind stress coefficient over water surfaces. Journal of Geophysical Research 85, 433–442.

Aeschbach-Hertig, W., Holzner, C.P., Hofer, M., Simona, M., Barbieri, A., Kipfer, R., 2007. A time series of environmental tracer data from deep, meromictic Lake Lugano, Switzerland. Limnology and Oceanography 52, 257–273.

Burger, D.F., Hamilton, D.P., Pilditch, C.A., 2008. Modelling the relative importance of internal and external nutrient loads on water column nutrient concentrations and phytoplankton biomass in a shallow polymictic lake. Ecological Modelling 211, 411–423.

Cole, J.J., Prairie, Y.T., Caraco, N.F., McDowell, W.H., Tranvik, L.J., Striegl, R.G., Duarte, C.M., Kortelainen, P., Downing, J.A., Middelburg, J.J., Melack, J., 2007. Plumbing the global carbon cycle: integrating inland waters into the terrestrial carbon budget. Ecosystems 10, 171–184.

Cole, J.J., Pace, M.L., Carpenter, S.R., Kitchell, J.F., 2000. Persistence of net heterotrophy in lakes during nutrient addition and food web manipulations. Limnology and Oceanography 45, 1718–1730.

Coloso, J.J., Cole, J.J., Hanson, P.C., Pace, M.L., 2008. Depth-integrated, continuous estimates of metabolism in a clear-water lake. Canadian Journal of Fisheries and Aquatic Sciences 65, 712–722.

Fee, E.J., Hecky, R.E., Kasian, S.E.M., Cruikshank, D.R., 1996. Effects of lake size, water clarity, and climatic variability on mixing depths in Canadian Shield lakes. Limnology and Oceanography 41, 912–920.

Ferris, J.M., Burton, H.R., 1988. The annual cycle of heat-content and mechanical stability of Deep Lake, Vestfold Hills, Antartica. Hydrobiologia 165, 115–128.

Gaiser, E.E., Deyrup, N.D., Bachmann, R.W., Battoe, L.E., Swain, H.M., 2009. Effects of climate variability on transparency and thermal structure in subtropical, monomictic Lake Annie, Florida. Fundamental and Applied Limnology Archiv für Hydrobiologie 175, 217–230.

Hambright, K.D., Gophen, M., Serruya, S., 1994. Influence of long-term climatic changes on the stratification of a subtropical, warm monomictic lake. Limnology and Oceanography 39, 1233–1242.

Hanson, P.C., Carpenter, S.R., Armstrong, D.E., Stanley, E.H., Kratz, T.K., 2006. Lake dissolved inorganic carbon and dissolved oxygen: changing drivers from days to decades. Ecological Monographs 76, 343–363.

Hanson, P.C., 2007. A grassroots approach to sensor and science networks. Frontiers in Ecology and the Environment 5, 343.

Hicks, B.B., 1972. Some evaluations of drag and bulk transfer coefficients over water bodies of different sizes. Boundary-Layer Meteorology 3, 201–213.

Hutchinson, G.E., 1957. A Treatise on Limnology, vol. 1. John Wiley & Sons, Inc., New York.

Idso, S.B., 1973. On the concept of lake stability. Limnology and Oceanography 18, 681–683.

Imberger, J., 1985. The diurnal mixed layer. Limnology and Oceanography 30, 737–770.

Imberger, J., Patterson, J.C., 1990. Physical limnology. Advances in Applied Mechanics 27, 303–475.

Jellison, R., Romero, J.R., Melack, J.M., 1998. The onset of meromixis during restoration of Mono Lake, California: unintended consequences of reducing water diversions. Limnology and Oceanography 43, 706–711.

Kling, G.W., 1988. Comparative transparency, depth of mixing, and stability of stratification in lakes of Cameroon, West-Africa. Limnology and Oceanography 33, 27–40.

Lamont, G., Laval, B., Pawlowicz, R., Pieters, R., Lawrence, G.A., 2004. Physical mechanisms leading to upwelling of anoxic bottom water in Nitinat Lake, 8 p. In: 17th ASCE Engineering Mechanisms Conference, June 13–16, 2004. University of Delaware, Newark, Delaware, EEUU.

Landsea, C.W., Vecchi, G.A., Bengtsson, L., Knutson, T.R., 2010. Impact of duration thresholds on Atlantic tropical cyclone counts. Journal of Climate 23, 2508–2519.

MacIntyre, S., Melack, M., 2009. Mixing dynamics in lakes across climatic zones. In: Likens, G.E. (Ed.), Encyclopedia of Inland Waters. Elsevier, Amsterdam, pp. 603–612.

MacIntyre, S., Flynn, K.M., Jellison, R., Romero, J.R., 1999. Boundary mixing and nutrient fluxes in Mono Lake, California. Limnology and Oceanography 44, 512–529.

MacIntyre, S., Fram, J.P., Kushner, P.J., Bettez, N.D., O'Brien, W.J., Hobbie, J.E., Kling, G.W., 2009. Climate-related variations in mixing dynamics in an Alaskan arctic lake. Limnology and Oceanography 54, 2401–2417.

MacIntyre, S., Romero, J.R., Kling, G.W., 2002. Spatial-temporal variability in surface layer deepening and lateral advection in an embayment of Lake Victoria, East Africa. Limnology and Oceanography 47, 656–671.

Magnuson, J.J., Kratz, T.K., Allen, T.F., Armstrong, D.E., Benson, B.J., Bowser, C.J., Bolgrien, D.W., Carpenter, S.R., Frost, T.M., Gower, S.T., Lillesand, T.M., Pike, J.A., Turner, M.G., 1997. Regionalization of long-term ecological research (LTER) on north temperate lakes. Internationale Vereinigung für Theoretische und Angewandte Limnologie Verhandlungen 26, 522–528.

Magnuson, J.J., Robertson, D.M., Benson, B.J., Wynne, R.H., Livingstone, D.M., Arai, T., Assel, R.A., Barry, R.G., Card, V., Kuusisto, E., Granin, N.G., Prowse, T.D., Stewart, K.M., Vuglinski, V.S., 2000. Historical trends in lake and river ice cover in the Northern Hemisphere. Science 289, 1743–1746.

Martin, J.L., McCutcheon, S.C., 1999. Hydrodynamics and Transport for Water Quality Modeling. Lewis Publ., New York.

McGowan, H.A., Sturman, A.P., 1996. Regional and local scale characteristics of foehn wind events over the South Island of New Zealand. Meteorology and Atmospheric Physics 58, 151–164.

Millero, F.J., Poisson, A., 1981. International one-atmosphere equation of state of seawater. Deep-Sea Research 28A 625–628.

Moberg, A., Sonechkin, D.M., Holmgren, K., Datsenko, N.M., Karlén, W., 2005. Highly variable Northern Hemisphere temperatures reconstructed from low- and high-resolution proxy data. Nature 433, 613–617.

Monismith, S.G., MacIntyre, S., 2009. The surface mixed layer in lakes and reservoirs. In: Likens, G.E. (Ed.), Encyclopedia of Inland Waters. Elsevier, Amsterdam, pp. 568–582.

Monismith, S., 1986. An experimental study of the upwelling response of stratified reservoirs to surface shear-stresses. Journal of Fluid Mechanics 171, 407–439.

Porter, J.H., Nagy, E., Kratz, T.K., Hanson, P., Collins, S.L., Arzberger, P., 2009. New eyes on the world: advanced sensors for ecology. Bioscience 59, 385–397.

Robertson, D.M., Imberger, J., 1994. Lake Number, a quantitative indicator of mixing used to estimate changes in dissolved-oxygen. Internationale Revue der gesamten Hydrobiologie 79, 159–176.

Robertson, D.M., Ragotzkie, R.A., 1990. Changes in the thermal structure of moderate to large sized lakes in response to changes in air temperature. Aquatic Sciences 52, 360–380.

Romero, J.R., Jellison, R., Melack, J.M., 1998. Stratification, vertical mixing, and upward ammonium flux in hypersaline Mono Lake, California. Archiv für Hydrobiologie 142, 283–315.

Rueda, F., Schladow, G., 2009. Mixing and stratification in lakes of varying horizontal length scales: scaling arguments and energy partitioning. Limnology and Oceanography 54, 2003–2017.

Schmidt, W., 1928. Über Temperatur and Stabilitätsverhaltnisse von Seen. Geographiska Annaler 10, 145–177.

Shintani, T., de la Fuente, A., Nino, Y., Imberger, J., 2010. Generalizations of the Wedderburn Number: parameterizing upwelling in stratified lakes. Limnology and Oceanography 55, 1377–1389.

Stevens, C.L., Lawrence, G.A., 1997. Estimation of wind-forced internal seiche amplitudes in lakes and reservoirs, with data from British Columbia, Canada. Aquatic Sciences 59, 115–134.

Thompson, R.O.R.Y., Imberger, J., 1980. Response of a numerical model of a stratified lake to wind stress. In: Proc. 2nd Int. Symp. Stratified Flows, Trondheim, June 1980. vol. 1, pp. 562–570.

Verburg, P., Hecky, R.E., Kling, H., 2003. Ecological consequences of a century of warming in Lake Tanganyika. Science 301, 505–507.

Wetzel, R.G., 1983. Limnology, first ed. Saunders College Publishing, Fort Worth.

Williamson, C.E., Saros, J.E., Vincent, W.F., Smol, J.P., 2009. Lakes and reservoirs as sentinels, integrators, and regulators of climate change. Limnology and Oceanography 54, 2273–2282.

Wüest, A., Lorke, A., 2003. Small-scale hydrodynamics in lakes. Annual Review of Fluid Mechanics 35, 373–412.